https://doi.org/10.5194/tc-2020-228
Preprint. Discussion started: 21 September 2020


The Cryosphere Discussions

# Modelling steady states and the transient response of debris-covered glaciers

James Ferguson[1] and Andreas Vieli[1]

[1]Glaciology and Geomorphodynamics Group, Institute of Geography, University of Zurich

**Correspondence:** James Ferguson (james.ferguson@geo.uzh.ch)

**Abstract.** Debris-covered glaciers are commonly found in alpine landscapes of high relief and play an increasingly important role in a warming climate. As a result of the insulating effect of supraglacial debris, their response to changes in climate is less direct and their dynamic behaviour more complex than for debris-free glaciers. Due to a lack of observations, here we use numerical modelling to explore the dynamic interactions between debris cover and glacier evolution over centennial timescales. The main goal of this study is to understand the effects of debris cover on the glacier's transient response. To do so, we use a numerical model that couples ice flow, debris transport and its insulating effect on surface mass balance and thereby captures dynamic feedbacks that affect the volume and length evolution. In a second step we incorporate the effects of cryokarst features such as ice cliffs and supraglacial ponds on the dynamical behaviour. Our modelling indicates that thick debris cover delays both the volume response and especially the length response to a warming climate signal. Including debris dynamics therefore results in glaciers with extended debris-covered tongues and that tend to advance or stagnate in length in response to a fluctuating climate and hence remember the cold periods more than the warm. However, when including even a relatively small amount of melt enhancing cryokarst features in the model, the length is more responsive to periods of warming and results in substantial mass loss and thinning on debris covered tongues, as is also observed in remote sensing.

## 1 Introduction

Debris-covered glaciers are commonly found in alpine landscapes of high relief, often when a primary source of mass input to the glacier comes from avalanching. Steep headwalls and slopes deliver debris consisting of loose rocks onto the glacier surface, mixed in with ice and snow. This debris becomes entrained in the ice and emerges on the surface further down-glacier in the ablation zone after it is left behind as the ice melts.

A debris-covered glacier is commonly defined as any glacier with a continuous debris cover across its full width for some portion of the glacier (Kirkbride, 2011). For a thin layer of debris, the resulting decrease in surface albedo leads to an elevated melt rate of the underlying ice; however, when the debris cover exceeds a thickness of a few centimetres, it reduces the ablation of the underlying ice (Østrem, 1959; Nicholson and Benn, 2006). For highly debris-covered glaciers, this reduced melt

https://doi.org/10.5194/tc-2020-228
Preprint. Discussion started: 21 September 2020


rate leads to glaciers with larger volumes and greater extents than would be expected for the corresponding debris-free case (Scherler et al., 2011).

Debris-covered glaciers exhibit a wide range of responses to changes in climate, some of which are counterintuitive (Scherler et al., 2011). Many debris-covered glaciers globally are retreating, particularly in the Himalayas (Bolch et al., 2012), though more slowly and with stagnant termini. Additionally, some debris-covered glaciers exhibit mass loss rates that are similar to those observed for nearby debris-free glaciers (Kääb et al., 2012; Gardelle et al., 2013; Pellicciotti et al., 2015; Brun et al., 2018) and that have been related to enhanced thinning rates on their debris covered glacier tongues. The formation of cryokarst features, such as ice cliffs and supraglacial ponds, has been suggested as a potential explanation for this anomalous thinning and therefore the occurrence of such features and their enhancing effect on surface melt have been intensively studied (Sakai et al., 2000, 2002; Steiner et al., 2015; Buri et al., 2016; Miles et al., 2016). However, the influence of dynamic effects on the thinning rates and glacier evolution has so far largely been neglected and such dynamic effects remain poorly understood. Further, from the reduction in ablation on debris covered glaciers a more delayed and dampened response is expected (Benn et al., 2012). Ideally one would use observational data across a greater temporal and geographical spectrum so that process feedbacks can be observed and examined over relevant time scales. However, the relatively recent advent of remote sensing data means that we have severe constraints on the availability of such long observational time series and the recent reconstruction of Zmuttgletscher (Mölg et al., 2019) provides the only observable record of a debris covered glacier that goes beyond a century.

Given the paucity of longterm data it is therefore essential to use advanced numerical models in order to investigate the role of glacier dynamics on glacier evolution and mass loss, allowing for the study of interacting processes over longer timeframes. Recent progress with numerical simulations of debris-covered glaciers include Konrad and Humphrey (2000), Vacco et al. (2010), Banerjee and Shankar (2013), Rowan et al. (2015), Anderson and Anderson (2016) and Anderson et al. (2019a). However, to date no study has used a coupled ice flow-debris transport model to study in detail the transient response and characteristic response times of a debris-covered glacier. This study aims to fill this gap by investigating the difference in transient response of debris-covered glaciers from their debris-free counterparts. In particular, we focus on the volume and length response to a fluctuating climate signal and the impact of including cryokarst features, such as ice cliffs and supraglacial ponds, on mass loss and surface evolution.

## 2 Methods

### 2.1 Governing equations

In order to examine the essential features of the interaction between glacier dynamics and debris cover, we couple an ice flow model to a debris transport model that includes both the debris melt-out and its insulating effect on ice ablation. In this model, the debris evolution affects the geometry and ice flow through changes in the surface mass balance. Our model is similar to that used in Anderson and Anderson (2016) with the main differences being some simplifications in the description of the ice

https://doi.org/10.5194/tc-2020-228
Preprint. Discussion started: 21 September 2020


flow, no explicit englacial debris tracking within the ice, and the novel option of melt enhancement due to cryokarst features. This cryokarst component is coupled to the flow dynamics and switches on when the tongue becomes stagnant.

### 2.1.1 Ice dynamics

For ice flow, we use a flowline version of the Shallow Ice Approximation (SIA), a simple model that allows for a realistic qualitative study of a glacier's response to changing climatic condition. The SIA has been used for studying glacier evolution and response times for debris-free glaciers (e.g., Leysinger Vieli and Gudmundsson, 2004), where it achieved comparable results to a full-Stokes solver with significantly less computational time. For a glacier with evolving ice thickness $H(x,t)$ flowing along the down-glacier direction $x$ with depth averaged velocity $\bar{u}(x,t)$ in response to a surface mass balance forcing $a(x,t)$, the equations for the thickness evolution and SIA ice flow are given by:

$$\frac{\partial H}{\partial t} + \frac{\partial(\bar{u}H)}{\partial x} = a, \tag{1}$$

$$\bar{u} = \frac{2A(\rho g)^n}{n+2} H^{n+1} \left|\frac{\partial h}{\partial x}\right|^{n-1} \frac{\partial h}{\partial x}, \tag{2}$$

where $\rho$ is the density of ice, $g$ is gravitational acceleration, $A$ and $n$ are the rate factor and exponent from Glen's flow law, respectively, and $h(x,t) = H + b$ is the glacier surface elevation for a given a bed elevation $b(x)$. The boundary conditions for the ice thickness $H$ are handled by specifying a Dirichlet or Neumann boundary condition at $x = 0$ and requiring that $H$ goes to zero at the glacier terminus, where the ice front position is a free boundary.

### 2.1.2 Debris dynamics

We assume that debris is homogeneously distributed within the ice with a spatially constant concentration $c$. The debris melts out when the ice melts at the surface and remains on the surface, where it is passively advected with the surface ice flow velocity $u_s = \frac{n+2}{n+1}\bar{u}$, until it reaches the terminus. The evolution of surface debris thickness $D(x,t)$ is represented by:

$$\frac{\partial D}{\partial t} + \frac{\partial(u_s D)}{\partial x} = \phi, \tag{3}$$

where $\phi$ is the debris source term at the surface given by

$$\phi(a,H) = \begin{cases} 0, & \text{if } a \geq 0 \\ -ca, & \text{if } a < 0 \end{cases}. \tag{4}$$

Note that for simplicity, we do not account for debris volume changes during melt due to density differences and debris porosity, hence our formulation is different by a constant factor compared to Naito et al. (2000) and Anderson and Anderson (2016).

https://doi.org/10.5194/tc-2020-228
Preprint. Discussion started: 21 September 2020


The Cryosphere Discussions
Open Access
EGU

#### 2.1.3 Surface mass balance

We assume that debris-free ice has an elevation dependent surface mass balance $\tilde{a}$ given by

$$\tilde{a}(z) = \min\{\gamma(H + b - \mathrm{ELA}), a_{max}\}, \tag{5}$$

where $\gamma$ is the mass balance gradient, ELA is the equilibrium line altitude, and $a_{max}$ is a maximum mass balance, which limits the accumulation to physically realistic values at very high elevations. A surface layer of debris enhances ice ablation when its thickness $D$ is below a threshold $D_0$. We neglect the effect of enhanced ablation when $D < D_0$ and represent the inverse relationship of surface mass balance with debris thickness (Nicholson and Benn, 2006) as

$$a = \tilde{a}\frac{D_0}{D_0 + D}. \tag{6}$$

#### 2.1.4 Debris boundary condition at glacier front

Supraglacial debris that covers the glacier throughout the ablation zone leaves the system via a terminal ice cliff, as typically observed at termini of debris covered glaciers (Ogilvie, 1904, see Fig A1 in the appendix). Such an ice cliff with non-zero velocity is important for debris being removed from the system as otherwise there is a physically unrealistic piling up of debris at terminus. The location of the terminal ice cliff is given by the point at which ice thickness $H$ reaches a critical thickness $H^*$. All debris melted out or transported past this point is assumed to slide off of the glacier relatively quickly and therefore does not play a role in the surface mass balance. This implies that the glacier will always have a small debris-free cliff area at the terminus with clean ice melt. The terminal boundary condition is similar to the one implemented in Anderson and Anderson (2016). For more details, see the appendix.

#### 2.1.5 Terminus cryokarst features

For some experiments, we use a simple and somewhat ad-hoc melt enhancement effect from ice cliffs and supraglacial ponds (denoted here as cryokarst features) that is coupled to ice dynamics. Observations indicate that ice cliffs and supraglacial ponds commonly occur near the termini of stagnating debris-covered glaciers (Pellicciotti et al., 2015; Brun et al., 2016) and are associated with regions that have low driving stresses. Using such a dynamic coupling as a first approximation, we couple the initiation of cryokarst features to driving stresses below a threshold value. Specifically, we define two driving stress thresholds, a maximum $\tau_d^+$ and a minimum $\tau_d^-$ and we introduce a local cryokarst area fraction $\lambda$ which represents the debris-free area associated with ice cliffs and supraglacial ponds. For a driving stress above $\tau_d^+$, the local cryokarst area fraction $\lambda$ is set to zero, which corresponds to no ice cliffs and no supraglacial lakes. For a driving stress below $\tau_d^-$, the local cryokarst area fraction equals a maximum value $\lambda_m$. For driving stress values in between the thresholds, we assume the local cryokarst contribution is linear in $\lambda$, given by

$$\lambda = \begin{cases} 0, & \text{if } \tau_d^+ \leq \tau_d \\ \lambda_m(\tau_d^+ - \tau_d)/(\tau_d^+ - \tau_d^-), & \text{if } \tau_d^- < \tau_d < \tau_d^+ \\ \lambda_m, & \text{if } \tau_d \leq \tau_d^- \end{cases}. \tag{7}$$

https://doi.org/10.5194/tc-2020-228
Preprint. Discussion started: 21 September 2020


For the fraction of area where cryokarst is present, we assume that there is no longer an insulating effect on the surface mass balance. Adjusting the local surface mass balance $a$ to account for this gives

$$a = \lambda\tilde{a} + (1-\lambda)\tilde{a}\frac{D_0}{D_0 + D}. \tag{8}$$

The threshold values $\tau_d^+$ and $\tau_d^-$ are based on the values of the driving stress during advance and retreat in the cryokarst–free case and are chosen such that $\tau_d$ only drops below the upper threshold $\tau_d^+$ once the glacier begins to stagnate during retreat, with realistic values taken to be $\tau_d^+$ between 100 and 125 kPa and $\tau_d^-$ between 50 and 75 kPa. For more details, see the appendix.

#### 2.1.6 Model setup numerical implementation

The coupled dynamic system described above is solved using standard finite differences and discretizations for the ice flow, similar to that first described by Mahaffy (1976), coupled with centred differences for the debris transport. Care is taken to ensure that each time step fulfills the CFL condition. Importantly, the boundary condition at the glacier terminus requires interpolation to determine the exact location of the critical ice thickness $H^*$ and to weight the surface mass balance forcing accordingly in the corresponding grid cell. Additionally, to avoid unwanted effects due to the steep gradient of the ice surface in SIA near the terminus which results in an unphysical drop in velocity, the velocity field in the vicinity of the terminus is adjusted by taking the mean velocity from the region upglacier averaged over ten ice thicknesses (here about 300 m), calculated using second order backward differencing.

In the results that follow, all computations are performed using a bed consisting of a headwall with a slope of 45° followed by a linear bed with slope of roughly 6°. All model constants are shown below in Table 2.

## 3 Modelling results

Our goal is to better understand how the transient response of a debris-covered glacier is different than that of a debris-free glacier and what effect cryokarst features have on this transient response. To do this, we perform a series of numerical experiments consisting of applying step changes or white noise histories in the climate forcing for glaciers with variable debris concentration and hence various levels of surface debris and analyze the resulting volume and length response. Table 1 gives an overview of the experiments with reference to the relevant figures in the text. Table 2 summarizes the parameter values used in the numerical model.

### 3.1 Steady state glacier extent

As a baseline for understanding the glacier's response to a changing climate, we first examine steady state features for the two climate extremes of our study, ELA = 3000 m and 3100 m. Although in reality, glaciers never attain a true steady state due to a constantly changing climate, equilibrium conditions are useful for theoretical studies because they provide well-understood rest states around which glacier fluctuations can be more easily studied. Figure 1 shows the glacier surface and bed profiles,

https://doi.org/10.5194/tc-2020-228
Preprint. Discussion started: 21 September 2020


The Cryosphere Discussions
Open Access
EGU

**Table 1.** Summary of modelling experiments performed.

| No. | Description | Section | Figures |
|---|---|---|---|
| 0 | Baseline: steady-states at ELA = 3000, 3100 m | 3.1 | 1 |
| 1 | Transient response due to step change between steady-states | 3.2 | 2,3,4 |
| 2 | White noise forcing | 3.3 | 5 |
| 3 | Transient response with cryokarst | 3.4 | 6 |
| 4 | White noise forcing with cryokarst | 3.5 | 7 |
| 5 | Advance-retreat from ELA = 3050 m to study terminus dynamics | 3.6 | 8 |

**Table 2.** Values used for the model parameters.

| Parameter | Name | Value | Units |
|---|---|---|---|
| ELA | Equilibrium line altitude | 3000 – 3100 | m |
| $\rho$ | Density of ice | 910 | kg m$^{-3}$ |
| $g$ | Gravitational acceleration | 9.80 | m s$^{-2}$ |
| $c$ | Debris volume concentration | 0 – 0.005 | |
| $A$ | Flow law parameter | 1 x 10$^{-24}$ | Pa$^{-3}$ s$^{-1}$ |
| $n$ | Glen's constant | 3 | |
| $D_0$ | Characteristic debris thickness | 0.05 | m |
| $a_{max}$ | Maximum surface mass balance | 2 | m yr$^{-1}$ |
| $\gamma$ | Surface mass balance gradient | 0.007 | yr$^{-1}$ |
| $H^*$ | Terminal ice thickness threshold | 30 | m |
| $\lambda_m$ | Maximum cryokarst fraction | 0 – 0.2 | |
| $dt$ | Time step | 0.01 | yr |
| $dx$ | Spatial discretization | 25 | m |
| $\tau_d^+$ | Upper cryokarst driving stress threshold | 100–125 | kPa |
| $\tau_d^-$ | Lower cryokarst driving stress threshold | 50–75 | kPa |
| $\theta$ | Bed slope | 0.1 | m m$^{-1}$ |
| $\theta_c$ | Headwall slope | 1 | m m$^{-1}$ |

velocity profiles, and debris thickness profiles for the debris-free case as well as for the debris concentrations of $c = 0.1, 0.25,$ and $0.5\%$. The glacier profiles in Fig. 1a and 1c show the expected behaviour of higher debris concentration leading to longer, larger glaciers. A debris concentration of only $0.1\%$ almost doubles the glacier length compared to the clean ice case. Note that the glacier geometry in the debris free part above the ELA is almost identical for all cases and hence independent of debris concentration. Surface velocities generally decrease with increasing debris thickness along the glacier, as seen in Fig. 1b and 1d.

https://doi.org/10.5194/tc-2020-228
Preprint. Discussion started: 21 September 2020




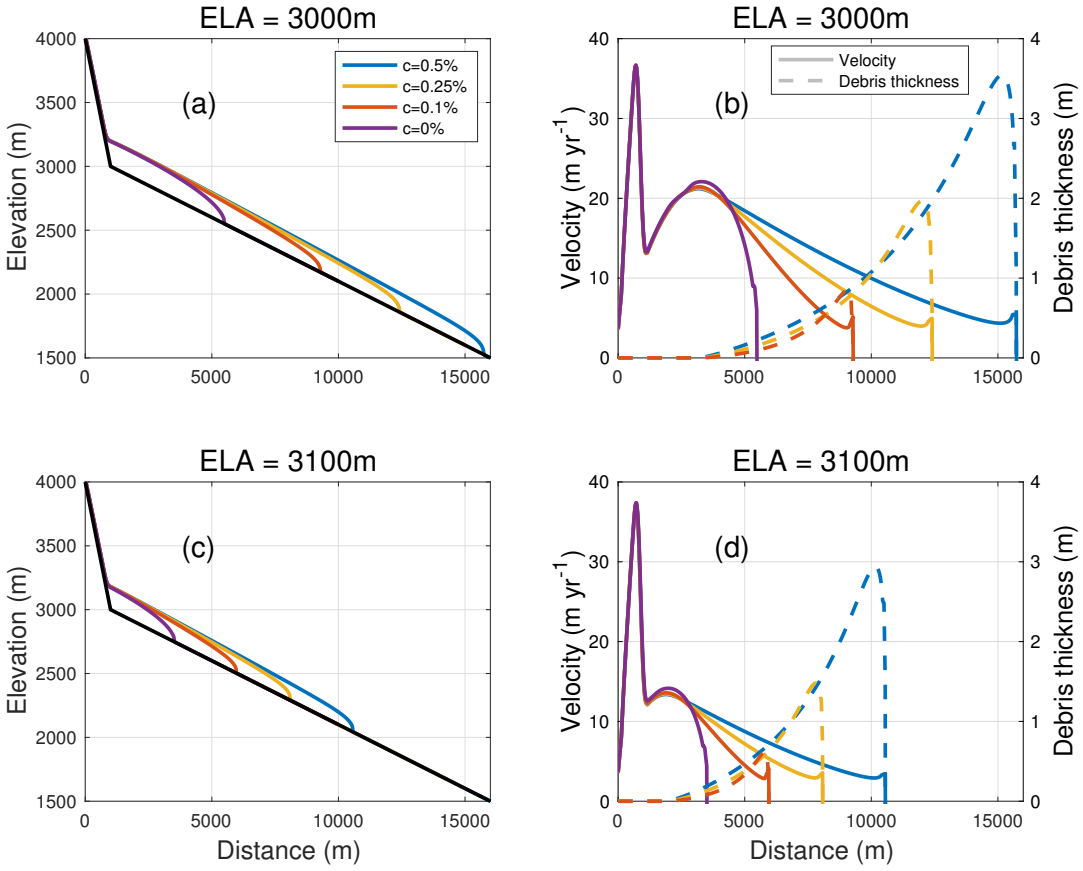


**Figure 1.** Steady state glacier geometry profiles (a and c), and profiles of surface velocity (solid lines) and debris thickness (dashed lines) (b and d), corresponding to ELA = 3000 m and 3100 m for four different debris concentrations.

An interesting observation here is that for a fixed climate, the debris thickness profile in steady state appears to be approx-
150 imately independent of concentration, while the glacier extents differ strongly. This is discussed further in Sec. 4.4.

### 3.2 Transient response between steady states

Next we analyze the response to a step change in the climate forcing. Figure 2 shows the transient volume and length changes due to ELA step changes of $\pm 100$ m. In Fig. 2b, glacier volume time series show the response time dependence on debris concentration, with the expected result that higher debris concentration leads to longer volume response time. Here, filled-in
155 squares denote the $e$-folding volume response time (Jóhannesson et al., 1989), which is the time it takes to reach $1-1/e \simeq 63\%$

https://doi.org/10.5194/tc-2020-228
Preprint. Discussion started: 21 September 2020


of the total volume change. The exact values of the numerical volume response time are shown in Table 3 in the columns marked $T_{num}$. In general, the volume response times are strongly increased for debris covered glaciers compared to the debris-free case. A more detailed discussion of volume response time follows in Section 4.3.

In Fig. 2c, the length times series allow for a comparison with the length response time. For the case of glacier advance, shown on the right side of the plot starting at $T = 1000$ years, the form of the length change is similar to that of the volume change: a slow but steady increase leading asymptotically to a steady state. However, the retreat phase, shown for $T = 0$ to 1000 yr, is contrasting this response behaviour. Here, we see a clear lag in length response, which gets stronger for larger debris concentrations. The lag is so pronounced that when the glaciers have reached their respective $e$-folding volumes, denoted as filled-in squares, they are still approximately at their pre-step change extent.

To show the difference in length versus volume response more clearly, we closely examine one debris-covered glacier, with $c = 0.25\%$ debris concentration, and contrast its response with the debris-free case. In Figure 3, the normalized volume and length are plotted together for each glacier, where we have set the cold (ELA = 3000 m) steady state volume $V = 1$ (length $L = 1$) and warm (ELA = 3100 m) steady state volume $V = 0$ (warm length $L = 0$) for ease of comparison. For the debris-free case, shown in Fig. 3a, the volume and length curves follow each other closely but there is a small but noticeable time lag between the volume response and the length response, which is more evident during retreat. The debris-covered response, in Fig. 3b, shows a substantial lag time between the volume response and the length response. This lag in the length response is, at roughly 250 years, much larger during the retreat but is also observable during the advance, where a 50 year lag is observed at the onset of advance. An additional difference between the glaciers is found near the end of the retreat phase. The transient debris-covered glacier volume overshoots the final steady state volume, observable starting just before $T = 500$ yr in Fig. 3b, before recovering to its final volume. During this overshoot and recovery in volume, the transient glacier length monotonically decreases and never goes below its final steady state length. In contrast, the transient debris-free glacier volume has no overshoots: it monotonically decreases during retreat.

In Figure 4, we again compare the debris-free case with the $c = 0.25\%$ debris-covered case but this time we look at the respective glacier thickness profiles during retreat. To facilitate comparison across spatial and temporal scales, we plot the normalized glacier thickness profiles for equivalent relative transient evolution times during retreat for both glaciers. In Fig. 4a, we see that immediately as the debris-free glacier thins, it also retreats in a roughly uniform way with thinning approximately matched by reduction in glacier extent. This can be thought of as a manifestation of a volume-area scaling law $V = cA^{\gamma}$ (e.g. Bahr et al., 1997), which essentially says that a debris-free glacier volume is linked to its area by a power law. The debris-covered glacier profile shown in Fig. 4b does not follow the same pattern. As the glacier thins during the period of relative time $\Delta t = 0$ to $\Delta t = 0.6$, there is no discernible change in the glacier extent. Initially, most of the thinning occurs in the upper half of the ablation zone but ceases there rapidly after $\Delta t = 0.1$ to 0.2 relative time. By $\Delta t = 0.6$, the entire region from relative length $x = 0$ to $x = 0.6$ is at or slightly below its final steady state ice thickness even though the original glacier extent has

https://doi.org/10.5194/tc-2020-228
Preprint. Discussion started: 21 September 2020


The Cryosphere Discussions

not changed yet. Only by $\Delta t = 0.8$ do we finally see the glacier terminus start to retreat, with the last roughly 35% of the glacier appearing as a thin, stagnating, and soon to be disconnected terminus (see Fig. S2 for corresponding stagnating velocity profiles). In the final 20% of the total retreat time, the stagnant terminus has completely disappeared and the central region that had previously over-thinned has now recovered to its steady state thickness and has become the new terminus. We revisit this interesting terminus behaviour in section 3.6 below.

**Table 3.** Comparison of numerical $e$-folding volume response times (in years) due to step changes between steady states at ELA = 3000 m and ELA = 3100 m for different debris concentrations. The columns marked $T_{num}$ represent the numerical volume response time and the other columns represent the theoretical estimate of Jóhannesson et al. (1989) developed for clean ice using different methods of calculating the surface mass balance at the terminus (see section 4.3 for details).

| | $\tau_v$ – retreat | | | | | $\tau_v$ – advance | | | | |
|---|---|---|---|---|---|---|---|---|---|---|
| $c$ | $T_{num}$ | $T_1$ | $T_2$ | $T_3$ | $T_4$ | $T_{num}$ | $T_1$ | $T_2$ | $T_3$ | $T_4$ |
| 0 | 77 | 52 | – | – | – | 133 | 108 | – | – | – |
| 0.1 | 154 | 29 | 456 | 54 | 222 | 265 | 48 | 694 | 87 | 340 |
| 0.25 | 256 | 22 | 646 | 42 | 207 | 396 | 34 | 955 | 66 | 321 |
| 0.5 | 385 | 17 | 800 | 34 | 179 | 529 | 25 | 1237 | 50 | 273 |

### 3.3 Response to white noise forcing

We have investigated debris-covered glacier response to step changes in the climate and it is natural to query whether these results will have any bearing on a more realistic fluctuating climate input. To investigate this issue in a somewhat less idealized setting, we initialize the model to a steady state corresponding to an ELA of 3050 m. Then we force the model using a varying climate signal consisting of a 5000 year long time series made up of random fluctuations between ELA = 3000 m and ELA = 3100 m which corresponds in the Alps to a change in air temperature of about $0.8°$C (Linsbauer et al., 2013). The fluctuations occur at fixed intervals of 100 years, which is close to but a bit larger than the clean ice response time during retreat, and they have a mean of ELA = 3050 m. This white noise ELA forcing is shown in Fig. 5a and the respective transient volume and length time series are shown in Fig. 5b and 5c for a debris-free glacier and three debris-covered glaciers with different debris concentrations.

The behaviour of the debris-free glacier (purple line at the bottom of Fig. 5b and 5c) exhibits a relatively rapid volume and length response, which can be seen by how quickly the solid curve, representing the transient, moves back towards the dashed line, which represents the steady state value for the mean climate of ELA = 3050 m. For the debris-covered glaciers with lower concentration (red and yellow lines in Fig. 5b), the volume responds only marginally more slowly. The difference is more pronounced for the glacier with the greatest debris concentration (blue line) where the transient volume never goes below the mean climate steady state volume beginning from $T = 2800$ yr. Note that the light blue shading corresponds to colder than

https://doi.org/10.5194/tc-2020-228
Preprint. Discussion started: 21 September 2020


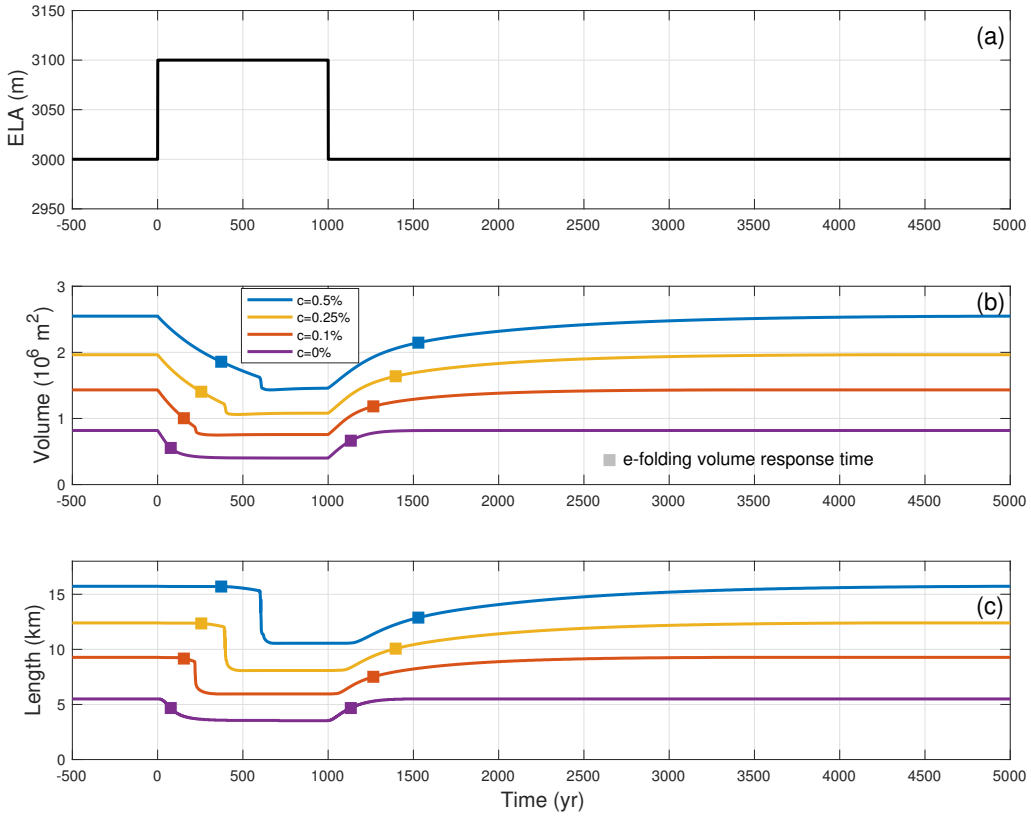


**Figure 2.** Step change in ELA between steady states (a) leading to transient volume response (b) and transient length response (c) for glaciers with different debris concentrations (coloured lines). The filled-in squares in both (b) and (c) represent the $e$-folding volume response time.

average time periods and white shading corresponds to warmer than average time periods.

The asymmetric response is much more pronounced in the transient length time series. While the glacier with the lowest debris concentration (red line in Fig. 5c), exhibits a marginally slower response compared to the debris-free case (solid purple line), the glaciers more heavily laden with debris, shown in yellow and blue, have transients lengths that are almost throughout more extended than the mean climate steady state length and tend to advance more than retreat. This is especially true for the $c = 0.5\%$ case, which after 5000 yr is more than 1 km longer than one would expect for the mean value climate. Hence, due to the lag in the length response to a warming climate, debris-covered glaciers preferentially show the effects of the colder climate. Put another way, debris-covered glaciers remember periods of cold climate more than warm ones.

https://doi.org/10.5194/tc-2020-228
Preprint. Discussion started: 21 September 2020


The Cryosphere Discussions
Open Access
EGU

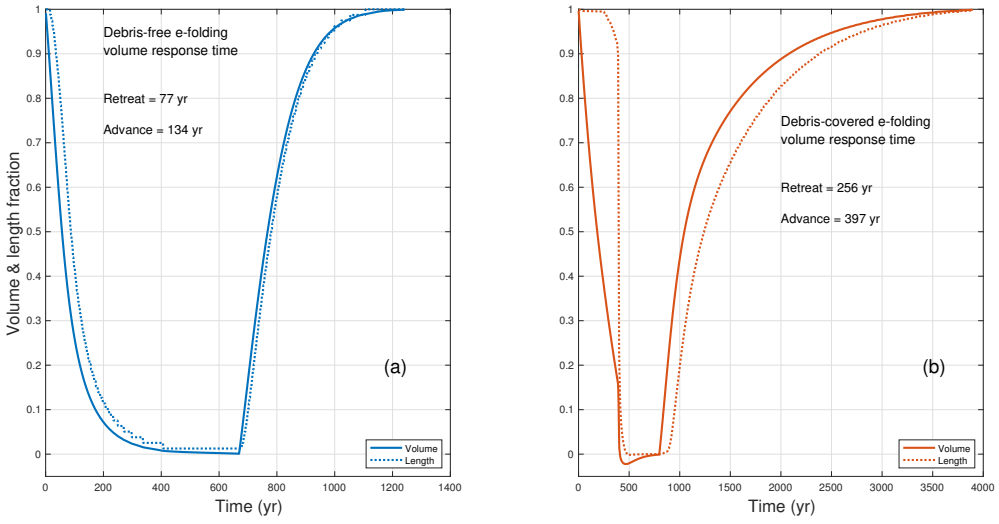


**Figure 3.** Normalized transient volume and length response for a step change in ELA between two steady states for (a) a debris-free glacier and (b) a debris-covered glacier with $c = 0.25\%$.

### 3.4 Effect of cryokarst on response

Most of the debris-covered glaciers observed in the present day have varying amounts of ice cliffs and supraglacial ponds present on their tongues which are known to enhance surface ablation. However, the long-term effect of such cryokarst features on thinning and glacier dynamics is poorly understood. With this in mind, we repeat the above experiments for four debris-covered glaciers, all with a medium debris concentration $c = 0.25\%$ by including the dynamic cryokarst model introduced in Section 2.1.5 and perform runs for different maximum local cryokarst area fraction of $\lambda_m = 0, 5, 10$, and $20\%$ using driving stress thresholds $\tau_d^+ = 110$ kPa and $\tau_d^+ = 60$ kPa. Since we dynamically couple the onset and intensity of melt enhancement from cryokarst to the driving stress using equations (7) and (8), the effect of cryokarst is only felt during periods of mass loss and we focus exclusively on this in Figure 6. The purple lines in Fig. 6a and 6b correspond to the case with no cryokarst features and therefore they show the same retreat as the yellow lines in Fig. 2b and 2c.

The addition of cryokarst has a noticeable effect on both the volume and length response of a debris-covered glacier. In Fig. 6a, there is a clear reduction in $e$-folding volume response time of a couple of decades visible (see Table 4 for the exact values), which is more pronounced with the presence of enhanced cryokarst. The effect on glacier length response is even more striking, with a difference of more than a century between the timings of the onset of retreat. The actual amount of equivalent bare ice for each glacier is shown as a percentage of the entire ablation zone area in Fig. 6c. Even for the smallest amount of cryokarst modelled, which accounts for only $2\%$ of equivalent bare ice in the ablation area, there is a shortening of roughly

https://doi.org/10.5194/tc-2020-228
Preprint. Discussion started: 21 September 2020


The Cryosphere
Discussions
Open Access
EGU

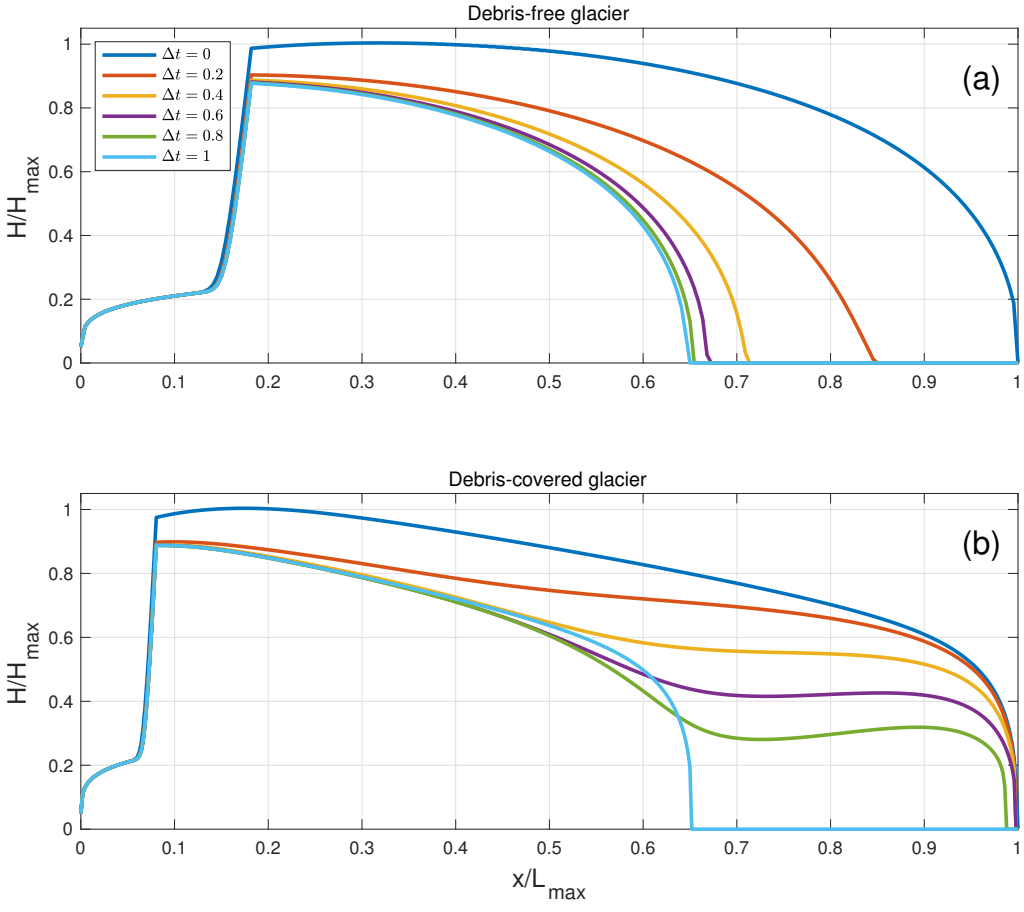


**Figure 4.** Glacier thickness profiles relative to the maximal initial thickness for (a) a debris-free glacier and (b) a debris-covered glacier with $c = 0.25\%$ at different times during a transient retreat. The different coloured lines refer to the time relative to the time it takes to retreat to steady state, where a time of $t = 0.1$ corresponds in the debris-free case to about 38 years and in the debris-covered case to about 40 years.

70 yr in the timing of the main phase of retreat. Despite this evident effect the presence of cryokarst has on length response, there is still a significant lag observed compared to the clean ice case, as in all modelled cases the glaciers are still at their maximum pre-step change extents even by the respective $e$-folding volume response times. Note that the choice of driving stress thresholds effects the strength of the cryokarst effect on the response (see Fig. S3 and S4 in the supplementary material).

https://doi.org/10.5194/tc-2020-228
Preprint. Discussion started: 21 September 2020


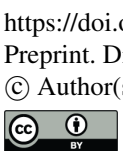

The Cryosphere
Discussions
Open Access
EGU

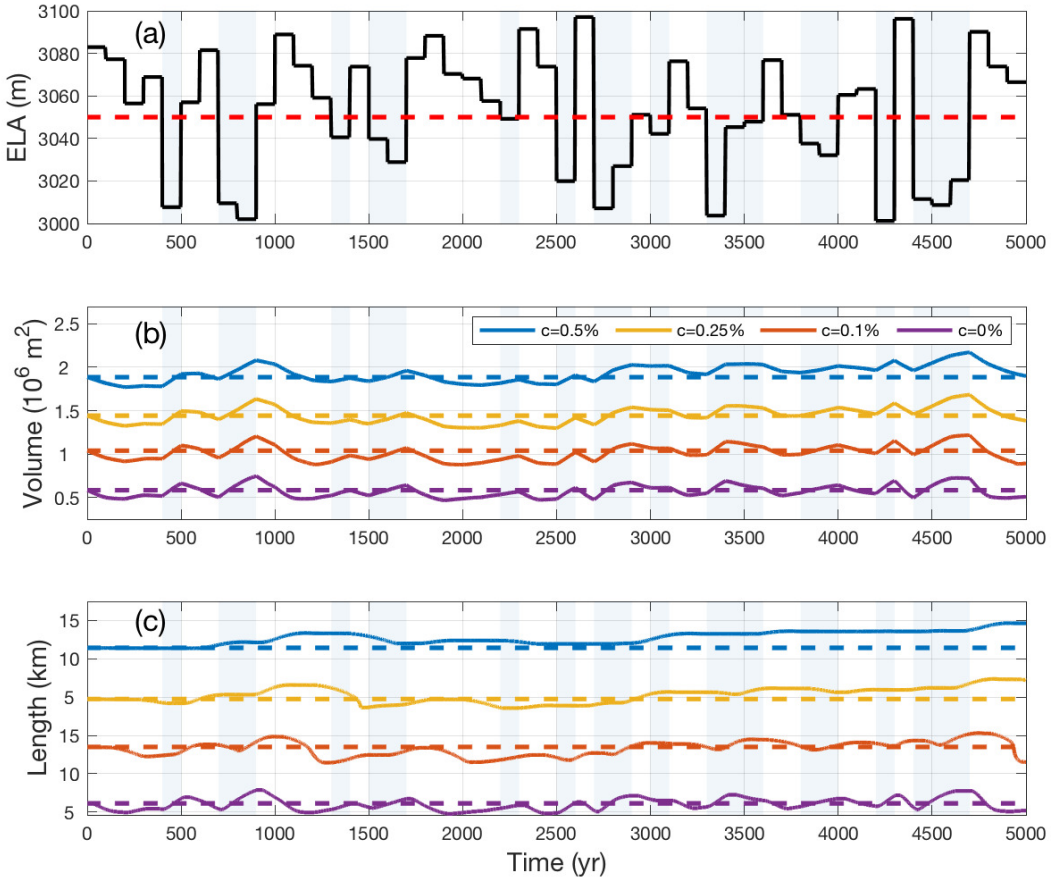


**Figure 5.** White noise climate forcing (a) and the corresponding transient volume response (b) and transient length response (c) for glaciers of different debris concentrations. The dashed lines represent (a) the mean value climate of ELA = 3050 m and the corresponding steady state (b) volume and (c) length. The light blue background shading represents temporal periods during which the climate forcing is colder than the mean climate.

### 3.5 Response to white noise forcing with presence of cryokarst

Figure 7 shows the same white noise forcing experiment with $c = 0.25\%$ as in Fig. 5 but with driving stress thresholds of $\tau_d^+ = 110$ kPa and $\tau_d^- = 60$ kPa, and four different maximum local cryokarst area fractions $\lambda_m = 0, 5, 10$, and $20\%$. As before, the $\lambda_m = 0$ glacier, corresponding to the purple curves in Fig. 7, is identical to the results already plotted in Fig. 5. in yellow. Since there is no dynamical effect during periods of advance, we do not see much difference in either the volume or length change rate in colder climate regimes; see in particular between 3000 and 5000 yr model time. However, during retreat the

https://doi.org/10.5194/tc-2020-228
Preprint. Discussion started: 21 September 2020


The Cryosphere Discussions

**Table 4.** Comparison of numerical $e$-folding volume response times (in years) due to step changes between ELA = 3000 m and ELA = 3100 m for a debris concentration of $c = 0.25\%$ and with the presence of several different values of maximum terminal cryokarst fraction $\lambda_m$.

| $c$ | $\lambda_m$ | $\tau_v$ |
|---|---|---|
| 0.25 | 0 | 256 |
| 0.25 | 0.05 | 234 |
| 0.25 | 0.1 | 219 |
| 0.25 | 0.2 | 200 |

difference is visible especially during the warm climate dominated period of $T = 1300$ to 3000 yr. In Fig. 7b and even more clearly in Fig. 7c, the transient volume and length of the cryokarst covered glaciers exhibit a shorter memory and are therefore able to retreat much more quickly than the corresponding cryokarst-free glacier. Despite this faster response, all of the modelled debris-covered glaciers still respond with much more delay than a debris-free glacier with the same climate forcing, as shown in the black dotted line in Fig. 7b and 7c, which has been rescaled in the magnitude for both length and volume for ease of comparison. As noted above, the timing in onset of retreat is rather sensitive to the choice of the upper and lower driving stress thresholds. To compare with results using different threshold values, please refer to supplementary figures S5 and S6.

### 3.6 Terminus behaviour during transient response

The results of our numerical experiments indicate that debris-covered glaciers have an asymmetric response to climate forcing, with a visible lag in response during a retreat, and that the magnitude of the lag is reduced in the presence of terminal cryokarst. To better understand this behaviour, we examine the debris-covered terminus region during advance and retreat and consider the relative magnitudes of surface mass balance $a$ and flux divergence $\partial Q/\partial x$ on the rate of thickness change $\partial H/\partial t$. Anderson et al. (2019a) used a similar approach to study thinning at the terminus but here we are primarily interested in the retreat rate. Fig. 8 shows the components of the mass conservation equation (1) for the moving region consisting of the last 200 m of debris-covered area for the cases of advance, retreat, and retreat with maximum local cryokarst area fraction $\lambda_m = 5\%$ and driving stress thresholds $\tau_d^+ = 110$ kPa and $\tau_d^- = 60$ kPa. The initial condition for all three panels is steady state for an ELA = 3050 m, with the advance and retreat due to ELA step changes of $\pm 50$ m at $T = 0$.

In each plot, the grey region represents the thickening or thinning rate, with the area under the curve representing the total thickness change of the last 200 m during the entire 1000 yr of the advance or retreat. In all three cases, during the first 200 yr the surface mass balance $a$, plotted in blue, does not change appreciably from the pre-step change value of $a = -0.2$ m yr$^{-1}$. This is because the debris at the terminus is thick enough to make the glacier here relatively insensitive to small changes in climate forcing. For the advancing glacier, depicted in Fig. 8a, the change in surface mass balance is minimal and the thickening rate is driven by an increase in the magnitude of the flux divergence (red line), that peaks at around $T = 150$ yr, the time taken

https://doi.org/10.5194/tc-2020-228
Preprint. Discussion started: 21 September 2020


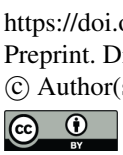

The Cryosphere
Discussions
Open Access
EGU

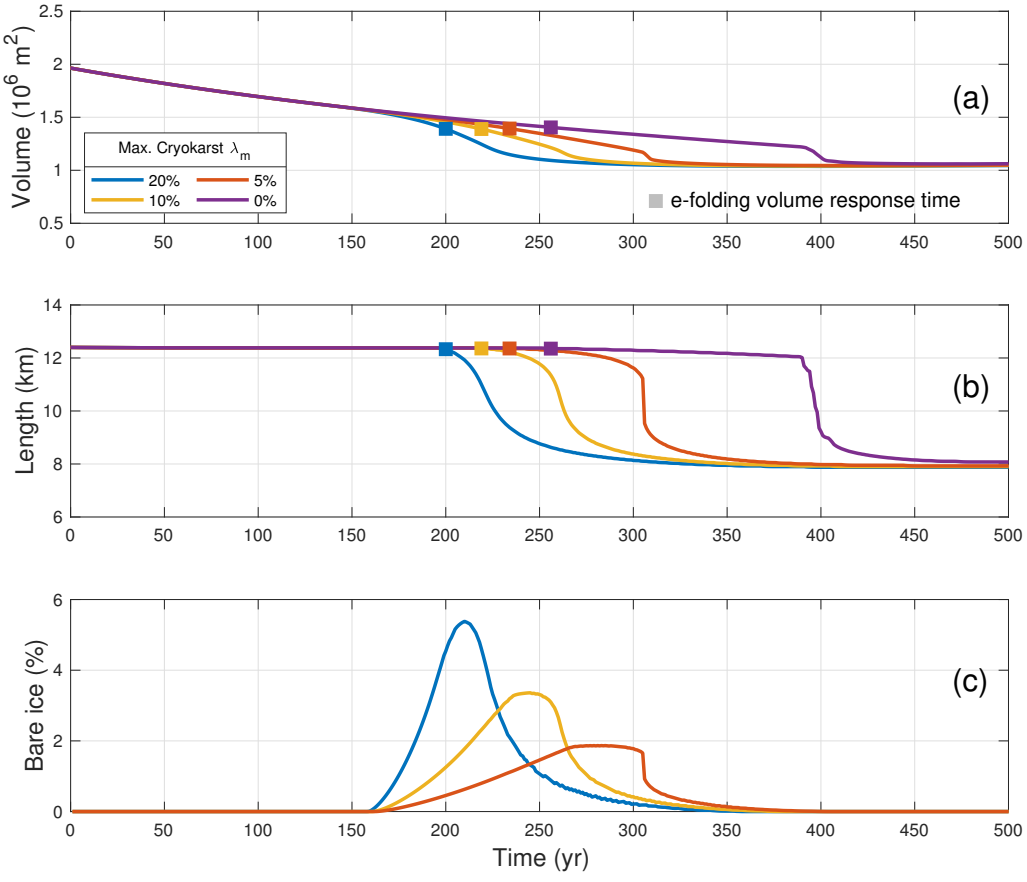


**Figure 6.** Transient volume response (a) and length response (b) for debris-covered glaciers with terminal cryokarst features retreating from steady state after a 100 m step change in ELA. Each colour represents a different value of the maximum cryokarst percentage $\lambda_m$. In all cases, the debris concentration is $c = 0.25\%$ and the driving stress thresholds are $\tau_d^+ = 110$ kPa and $\tau_d^- = 60$ kPa. The filled in squares in (a) and (b) represent the $e$-folding volume response time. The percentage of total debris-covered length that has a bare ice equivalent surface mass balance due to the presence of cryokarst is shown in (c).

for the increased ice flux to propagate down the glacier to the terminus.

For the retreating glacier, shown in Fig. 8b, the thinning rate is clearly driven by a decrease in flux divergence, which eventually drops to zero at roughly $T = 300$ yr, at which point the glacier terminus stagnated. It remains so until roughly $T = 500$ yr, when the total amount of thinning is large enough that the stagnant terminus finally disappears. After this, there is a small amount of thickening at the terminus as the glacier readjusts to the overshoot caused by the collapse of the stagnant terminus.

https://doi.org/10.5194/tc-2020-228
Preprint. Discussion started: 21 September 2020


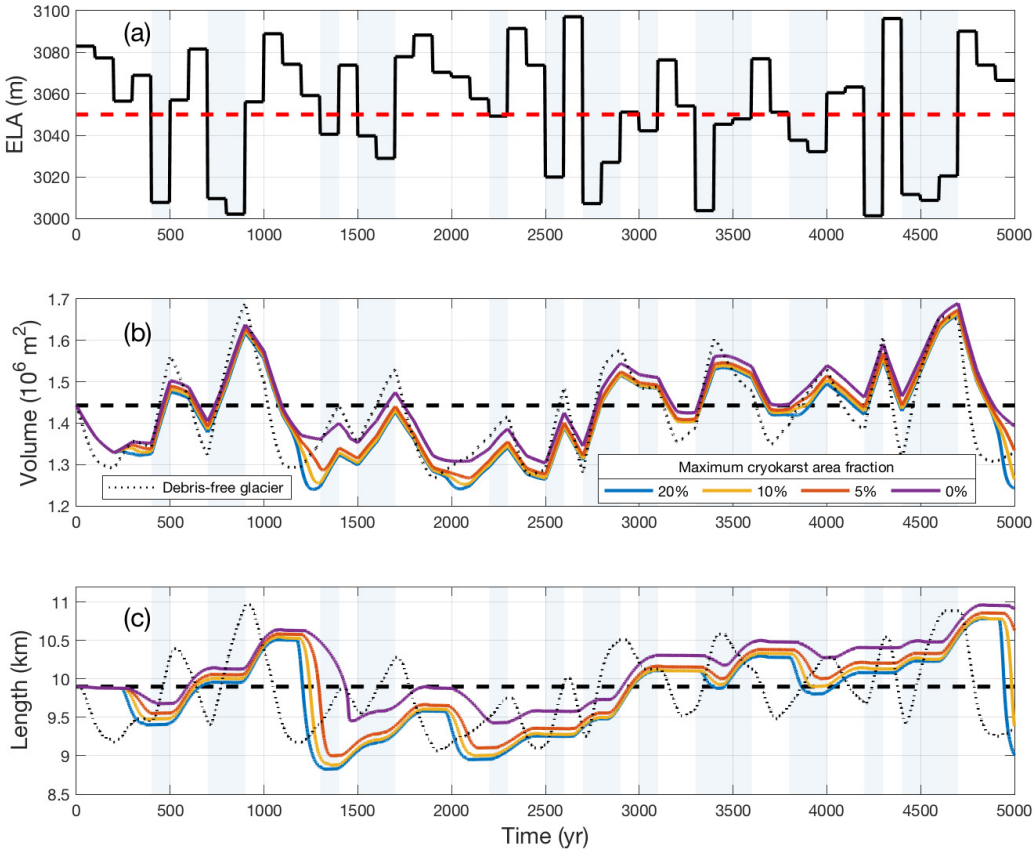


**Figure 7.** White noise climate forcing (a) and the corresponding transient volume response (b) and transient length response (c) for glaciers of different maximum cryokarst fraction $\lambda_m$. The dashed lines represent (a) the mean value climate of ELA = 3050 m and the corresponding steady state (b) volume and (c) length. The light blue background shading represents temporal periods during which the climate forcing is colder than the mean climate. In all cases, the debris concentration is $c = 0.25\%$ and the cryokarst driving stress thresholds are $\tau_d^+ = 110$ kPa and $\tau_d^- = 60$ kPa.

When a small amount of cryokarst features is added to the terminus during retreat, representing at most roughly 2% of the total debris-covered area (Fig 8c), the glacier behaves identically to the cryokarst–free case up until roughly $T = 190$ yr. From then on the terminus dynamics become stagnant enough that the cryokarst features begin to develop and within several decades cause an increase in the melt rate by a factor of more than two. This significantly speeds up the thinning on the tongue and hence the retreat rate, with the bulk of the retreat completed about 100 yr earlier than in the cryokarst–free case.

https://doi.org/10.5194/tc-2020-228
Preprint. Discussion started: 21 September 2020


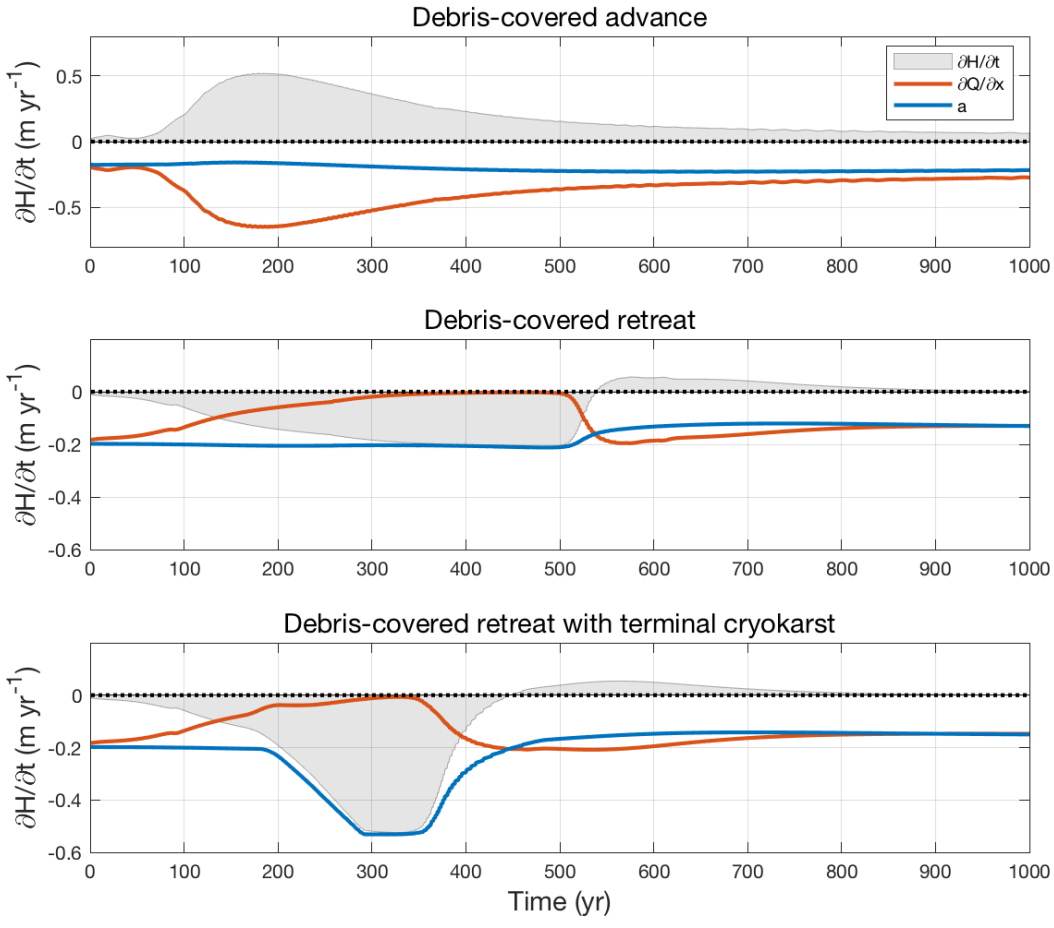


**Figure 8.** Thinning rate, flux divergence, and surface mass balance averaged over the final 200 m of the glacier terminus before the terminus during advance (a), retreat (b), and retreat with cryokarst (c), for $c = 0.25\%$, $\lambda_m = 0.05$, $\tau_d^+ = 110$ kPa, and $\tau_d^- = 60$ kPa. In all cases, the initial condition is a steady state at ELA = 3050 m followed by a 50 m step change in ELA at time $t = 0$.

## 4 Discussion

We explored the transient response of a debris-covered glacier to changes in climate forcing using a flowline model that couples ice flow with debris melt out and advection and also includes an ad-hoc representation of the effects of dynamically coupled cryokarst features at the glacier terminus. Several interesting results related to dynamics were obtained, which we discuss separately in light of observational data, previous studies, and model limitations.

https://doi.org/10.5194/tc-2020-228
Preprint. Discussion started: 21 September 2020


### 4.1 Debris-covered glacier memory

The memory of a debris-covered glacier was shown to be selective, exhibiting an effective hysteresis, with periods of relatively cold climate having a sustained effect on the volume and in particular on the length. Strictly speaking this is not a true hysteresis since if the glacier is allowed a lengthy relaxation period of several centuries, the resulting equilibrium is independent of history. The glacier termini seem to struggle to retreat in warmer periods even if they are sustained over a century, and hence debris covered glaciers have the tendency to either advance or stagnate in a fluctuating climate (Fig. 5). This also means that for debris covered glaciers, no unique glacier length exists for a given climate, but rather that the length of debris covered glaciers is determined by the history of repeated cold phases. This is a novel result which has important implications not only for the observed present day extended extents of debris-covered glaciers but also on historical reconstructions. For example, inferences of past climate from historical glacier extents that do not take into account the asymmetric memory of debris-covered glaciers risk misrepresenting the climate as being colder than it actually was.

Observational data (Quincey et al., 2009; Scherler et al., 2011; Ragettli et al., 2016) show that many debris-covered glaciers have strongly extended and stagnating tongues which is consistent with our modelling and our interpretation that debris-covered glaciers remember rather the colder climates of the past and are therefore quite far out of balance with the present climate. Note, that this asymmetric memory is much more pronounced for the adjustment in glacier length than in volume. However, since the observational record is not long enough to provide data on meaningful timescales and is heavily biased towards retreating glaciers, it is currently only possible to study this phenomenon fully using numerical experiments.

Note, that this asymmetric response to climate forcing is much more pronounced for the adjustment in glacier length than in volume. In the white noise experiments, volume change and hence average thinning behaviour are surprisingly similar for all debris concentrations and the clean ice case (Fig. 5), which agrees with the general observations of relatively high mass loss despite the occurrence of substantial debris cover (Pellicciotti et al., 2015; Brun et al., 2018). Such rapid mass loss is governed by two processes. Initially, the warming has a strong impact on the upper accumulation area where debris is still thin. Then the lower tongue with thick debris cover stagnates and dynamic ice replacement diminishes ($\partial Q/\partial x$ goes to zero, Fig. 8b) and hence the ice simply melt away. As this stagnant area is extensive the related total volume loss is therefore substantial.

The results presented used a white noise forcing with a particular ELA range and time interval between random step changes. Different climate forcing signals are possible, as are many different shapes and sizes of glaciers with varying debris thickness profiles. However, the general qualitative results are expected to be the same, though for example a longer time interval between random steps (approaching the debris-covered response time) will reduce the debris-covered memory effect. An obvious extension of this work is to undertake a detailed sensitivity analysis, using a variety of climate signals, glacier geometries, and debris thickness profiles, in order to better understand the conditions under which this selective memory effect becomes significant.

https://doi.org/10.5194/tc-2020-228
Preprint. Discussion started: 21 September 2020


### 4.2 Cryokarst effect in modulating response

Our results suggest that cryokarst features which dynamically develop during a retreat on the stagnating terminus substantially speed up the length response and also noticeably reduce the volume response time. This is important for any long-term modelling studies involving debris-covered glaciers, as neglecting the effects of cryokarst results in an overestimation of transient response times during a warming phase. Furthermore, the resulting earlier and more enhanced mass loss rates agree better with the current observations of rapid thinning (Pellicciotti et al., 2015; Brun et al., 2018; Mölg et al., 2019) but the terminus response is still strongly delayed and requires warm periods of substantial durations (several centuries) to cause substantial retreat (Fig. 7). This suggests that todays thinning may still be related to the warming after the Little Ice Age, or alternatively, it may be a consequence of our rather ad-hoc approach and threshold for the onset of cryokarst.

Numerous previous studies (Sakai et al., 2000, 2002; Benn et al., 2012; Buri et al., 2016; Miles et al., 2016; Ragettli et al., 2016; Rounce et al., 2018) have investigated the role of ice cliffs and supraglacial ponds on the enhancement of melt on debris-covered glaciers and indicate some link between stagnation in dynamics and the development of such cryokarst features. Our model is, however, the first attempt to couple the effects of these features to glacier dynamics and explore its impact on glacier thinning. Although the ad-hoc approach used here is admittedly simplistic, it does allow for the general effect of cryokarst to be incorporated dynamically without requiring knowledge of the details of the physical processes, which are not yet completely worked out and would greatly complicate the numerics since they are sub-grid scale. The parameters chosen resulted in behaviour consistent with fractional area observations (Mölg et al., 2019; Anderson et al., 2019b; Steiner et al., 2019, give a local area fraction up to 10%) and the approximate timing of the cryokarst evolution also matches the observation that stagnating glaciers tend to have more cryokarst (Benn et al., 2012).

The main limitation to this component of the model is that the choice of driving stress thresholds for the onset of cryokarst features is not well constrained by observations or directly linked to a sub-grid process based model. Hence it is clear that a better understanding of the link between glacier dynamics and the formation of cryokarst is needed and a more sophisticated model that faithfully represents the large scale, long-term effect of ice cliff and supraglacial pond evolution on the local surface mass balance would be useful for future studies.

### 4.3 Transient response time

The thinning and hence the volume response during retreat occurs in two distinct phases: a first relatively rapid response in the debris-free zone directly caused by enhanced melting, followed by a slower response in the debris-covered zone punctuated by the collapse of the stagnant terminus, and caused by the stagnation of the debris covered tongue. Although this has been indicated conceptually by general observations, Banerjee and Shankar (2013) gave the first dynamical explanation for this behaviour using a simplified representation of the effects of debris cover. Here we use a more physically realistic model which includes debris evolution coupled to the ice flow and our results confirm their dynamical explanation. An important implication

https://doi.org/10.5194/tc-2020-228
Preprint. Discussion started: 21 September 2020


of this result, also pointed out by Banerjee and Shankar (2013), is that a simple volume response time scale to characterize the transient response of a glacier to climate forcing, developed for debris-free glaciers in Jóhannesson et al. (1989) and Harrison et al. (2001), does not seem possible for debris-covered glaciers because of its more complicated retreat behaviour.

To illustrate this, we calculate for our step change experiments (Sec. 3.2) the theoretical volume response time of Jóhannesson et al. (1989), which is given by

$$\tau_v = \frac{H_m}{-a_t}, \tag{9}$$

where $H_m$ is the maximum ice thickness and $a_t$ is the surface mass balance at the glacier terminus. It is, however, not that clear how to define the terminal surface mass balance, as the glacier has both a debris-covered and a debris-free zone (frontal cliff) near the terminus. This is even more problematic when there is a zone of cryokarst at the terminus, so we neglect that case here. We choose four different terminus locations to extract the surface mass balance at the terminus from the modelling results and which depend on the location of extraction: for the response time $T_1$, the terminal surface mass balance is taken on the debris-free terminal ice cliff; for $T_2$, it is taken on the debris-covered zone just up-glacier from the ice cliff; for $T_3$, it is taken as an average of the surface mass balances from $T_1$ and $T_2$; and for $T_4$, it is taken from the average over the last 300 m (or roughly ten ice thicknesses) including the debris-free ice cliff. The results of these response time calculations for both retreat and advance are found in Table 3. As is evident by comparison with the corresponding numerical volume response times, none of these approaches gives reasonable theoretical predictions (Table 3) and results in either strongly over or underestimated response times, depending on whether the debris-free ice cliff is excluded. Note that using the theoretical volume response time of Harrison et al. (2001) does not make sense here, as this calculation takes into account the gradient of the surface mass balance near the terminus, which is close to zero wherever there is debris cover.

The presence and variability of debris cover brings into play additional dynamics that affect not only the volume response but also the geometry. The transient glacier thickness profile during a retreat showed two distinct shapes, depending on whether the stagnant and unsustainable tongue was still present. This time dependent glacier shape suggests that the volume–area power law scaling relationship that exists for debris-free glaciers (e.g. Bahr et al., 1997) is unlikely to exist in such a simple form for debris-covered glaciers. Volume–area scaling for debris-free glaciers, which rests on both theoretical arguments and observational data, shows that debris-free glaciers keep essentially the same shape even if they are not in steady state. This is clearly not true for the debris-covered glaciers modelled in our study.

Future work in establishing a way to understand and predict volume response times would be very beneficial here, as it would allow the approximate assessment of the large scale volume and length response to climate forcing without the need to run detailed, computationally expensive models for each glacier.

https://doi.org/10.5194/tc-2020-228
Preprint. Discussion started: 21 September 2020


### 4.4 Steady state velocity–debris thickness relationship

The steady state profiles resulting from our model show an inverse relationship between debris thickness and ice flow velocity, consistent with both observations (Mölg et al., 2019) and other numerical studies (Anderson and Anderson, 2016, 2018). It is natural to ask to what extent the debris thickness profile depends on the ice flow model and the debris transport model used. That question can be answered for the steady state case without assuming anything about the ice flow and considering only conservation of mass. In steady state and for the debris-covered domain, eqs. (1) and (3) can be written as one equation:

$$\kappa \frac{\partial(\bar{u}H)}{\partial x} + \frac{\partial(\bar{u}D)}{\partial x} = 0, \tag{10}$$

where $\kappa = cu_s/\bar{u}$. Integrating from the location of initial debris emergence (in our case the position of the ELA) to an arbitrary point $x$ further down glacier and rearranging, we obtain an expression for steady state debris thickness $D$ given by

$$D(x) = \frac{\kappa \bar{u}_e H_e}{\bar{u}} - \kappa H, \tag{11}$$

where $\bar{u}_e$ and $H_e$ are depth averaged ice velocity and ice thickness at the point of initial debris emergence, respectively. Near the terminus, the ice thickness $H(x)$ approaches zero and hence, the terminal debris thickness $D_{tr}$ can be expressed as

$$D_{tr} \simeq \frac{\kappa Q_e}{\bar{u}_{tr}}, \tag{12}$$

where $Q_e = \bar{u}_e H_e$ is the ice flux at the initial debris emergence point and $\bar{u}_{tr}$ is the ice velocity at the terminus. An interesting consequence is that for a debris-covered glacier near steady state with an approximately uniform debris concentration, one can infer this concentration by measuring the representative velocity and debris thickness at the terminus and the velocity and ice thickness at the emergence location.

An additional feature of these model results is that for a fixed climate, the debris thickness profile in steady state appears to be approximately independent of concentration. Although this agreement is not perfect, one can see that the dashed lines indicating debris thickness in panels Fig. 1b and 1d are within 10% of each other for most of the ablation zone. For example, the two glaciers present at $x = 10$ km both have a debris layer of about 1 m thick even though their respective debris concentrations differ by a factor of two. The exception is the upper ablation zone just below the position of debris emergence (e.g. ELA), as there debris thicknesses are very low and relative differences therefore large. The differences in this zone seems to have a profound impact on the downstream velocity and ice flux gradient and hence seem to govern the final steady state glacier length. The very similar debris thicknesses for all concentrations in the lower part of the tongue directly imply almost identical surface mass balance at the same locations (for surface mass balance profiles see Fig S1).

### 4.5 Model limitations

We have used a well-tested but relatively simple ice flow model, the shallow ice approximation, for our simulations rather than a full-Stokes model and it is important to understand how much this choice matters for the qualitative analyses performed in

https://doi.org/10.5194/tc-2020-228
Preprint. Discussion started: 21 September 2020


our study. For the case of debris-free glaciers, this question was examined in Leysinger Vieli and Gudmundsson (2004) and the finding was that there is little difference in response times between these two models and when interested in glacier evolution. We expect this result would also be true in our case, as the representation of debris transport in our model does not depend on the ice physics.

Our model did not resolve the englacial transport of debris and assumed that all debris immediately starts melting out at the ELA. This approximation is reasonable for debris that is deposited onto the glacier surface near the effective ELA But this assumption works less well for glaciers whose debris deposition zone is far above the ELA since the resulting emergence location will be located much further down glacier. However, this will likely not change any of our qualitative results but just shift the debris emergence location downstream from the ELA, resulting in the same general pattern of thickening of debris along the glacier and therefore essentially the same transient behaviour.

A more important issue is what happens at the terminus. In addition to the limitations of the cryokarst model discussed above, a further concern is the choice of boundary condition at the terminus. Our boundary condition is qualitatively similar to that used in Anderson and Anderson (2016), in that for both models there is a sub-grid scale rule for defining the interface between the debris-covered surface and an exposed ice terminus. The rare observations of advancing glaciers support the use of a terminal ice cliff (see Appendix) but during retreat this is less commonly observed. Even so, the boundary condition we use captures the effects of a stagnating tongue and therefore still seems largely consistent with observations of terminus dynamics. More detailed observations of the termini or debris-covered glaciers and their effect on the glacier dynamics would be of benefit for future modelling studies.

## 5 Conclusions

We have presented a model that captures the essential processes governing debris-covered glacier dynamics while in a second step also integrating the effect of evolving cryokarst features on glacier evolution. Using this model, we have investigated the transient response of debris-covered glaciers to changes in climate. The results show that for a retreat the length response is strongly delayed compared to the volume response and that in general volume response times are much longer than for clean ice glaciers. This implies that periods of cold climate have a longer lasting effect on the transient volume and particularly on the length of debris-covered glaciers than do periods of warm climate. Such glaciers therefore tend to advance or stagnate in length in a fluctuating climate and hence glacier length is not representative of climate but rather depends on the history of cold phases. The modelled extended but generally stagnant glacier tongues in a warming climate are in agreement with observations. With regard to volume loss, the model is however much more responsive and can produce similar to observed substantial thinning and hence mass loss on the extended tongues due to stagnation or more specifically the cessation in local dynamic replacement of ice.

https://doi.org/10.5194/tc-2020-228
Preprint. Discussion started: 21 September 2020


When cryokarst features are dynamically included in the model, it enhances both terminus thinning and the retreat rate and produces similar mass loss rates to those observed today. However, our cryokarst-model was rather simple and the related parameters not well constrained, underscoring the need for a better understanding of the evolution of ice cliffs and supraglacial ponds so that they may be more accurately represented in long-term modelling studies.

Currently existing theoretical volume response times do not appear to be relevant for debris-covered glaciers because there is not a consistent way to define the surface mass balance at the terminus that gives theoretical values that match the numerical response times. Taking into account only the debris-covered area greatly overestimates the response time and this is likely due to the more complicated dynamics caused by the presence of the debris layer.

*Code availability.* Code used to generate the analyses used in this study is available upon request.

## Appendix A: Boundary condition at the terminus

The choice of debris boundary condition near the terminus is not trivial, as many simple approaches lead to numerical simulations that exhibit unacceptable behaviours. Debris must leave the system before reaching the glacier terminus as otherwise the glacier can effectively grow without bound since debris may continue to thicken down-glacier indefinitely, thereby almost entirely insulating the glacier from melt. Hence, the debris boundary condition must be applied at a point up-glacier from the glacier terminus. However, boundary conditions that are defined at a location which depends on grid size, such as a fixed number of grid points from the glacier terminus, run the risk of exhibiting grid-size dependency in the numerical simulations. For example, we found that applying a debris flux condition one grid point from the glacier terminus results in a steady state glacier length that is heavily grid-size dependent, with the length varying by many times the mesh size. This is an undesirable outcome since the glacier physics should be independent of the numerical discretization used.

Observations of debris-covered glaciers that terminate in an exposed dynamically active ice cliff are numerous, occurring in relatively recent aerial images (e.g. Tsijiore Nouve, shown in Fig. A1a), early glaciological literature (Ogilvie, 1904), and even historical paintings (Escher von der Linth, 1794, as shown in Fig. A1b). Motivated by these observations, we define the point at which the debris leaves the glacier to coincide with the location $x^*$ of a terminal ice cliff of critical thickness $H^*$, as shown in Fig. A2. All the surface debris transported past the ice cliff location $x^*$ slides down the cliff and out of the system. Since the critical ice thickness will generally fall between two grid points, a sub-grid interpolation is performed to determine the exact location of the ice cliff and the surface mass balance of the cell containing the ice cliff is then defined as a weighted average of debris-covered and bare ice melt rates. This boundary condition is found to be grid size independent in the sense that it results in steady state glacier extents that converge to a constant value, within an error of less than the grid spacing.

https://doi.org/10.5194/tc-2020-228
Preprint. Discussion started: 21 September 2020




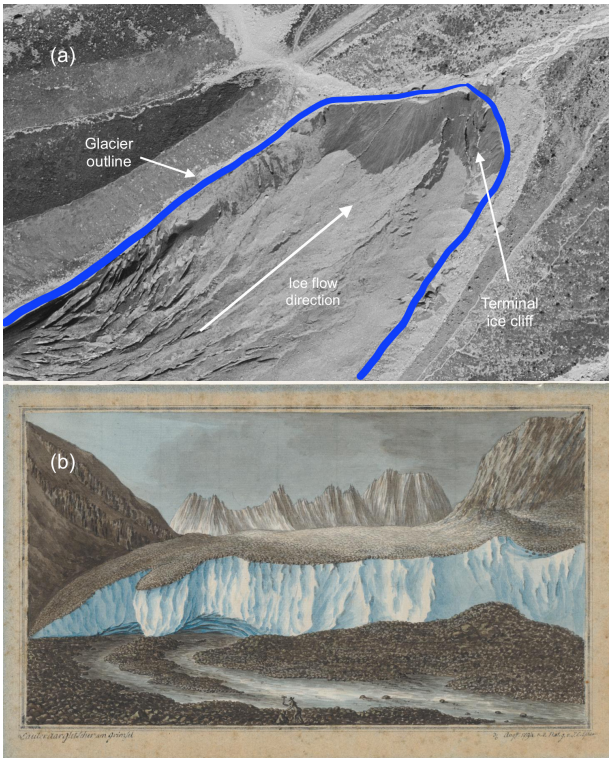


**Figure A1.** Examples of debris-covered glaciers with an ice cliff terminus: (a) satellite image of Tsijiore Nouve Glacier in 1988, reproduction with permission from Swisstopo (BA20059) and (b) a painting of the terminus of Unteraargletscher from 1794 (Escher von der Linth, 1794).

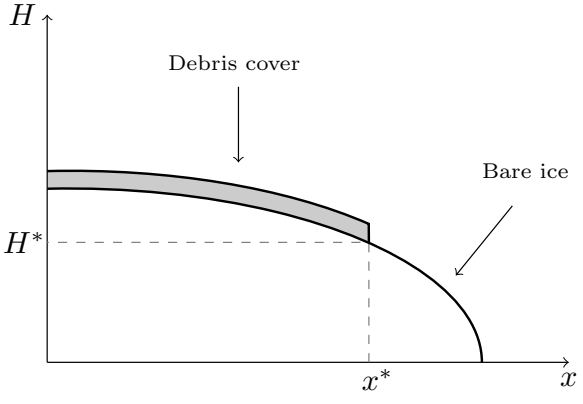


**Figure A2.** Schematic representation of the model terminus boundary condition. Debris covers the glacier only until a point $x^*$, corresponding to a critical glacier thickness $H^*$, and past this point the glacier is debris-free.

https://doi.org/10.5194/tc-2020-228
Preprint. Discussion started: 21 September 2020


## Appendix B: Cryokarst model

The model coupling cryokarst features to glacier dynamics described in Section 2.1.5 requires threshold values of driving stress, $\tau_d^+$ and $\tau_d^-$, that define the presence of cryokarst near the terminus, which in turn reduces the insulating effect of the debris locally. We choose the values of the thresholds by examining the modelled driving stress of a debris-covered glacier during retreat and choosing threshold values that seem consistent with the onset of stagnation. The upper threshold between 100 and 125 kPa is consistent with driving stresses observed at the upper limit of the cryokarst zone at Zmuttgletscher in the Alps during its retreat from the Little Ice Age to today (100 to 130 kPa; Mölg et al., 2020). In Fig. B1a, we plot $\tau_d$ at 50 yr intervals during retreat following a step change between two steady states at ELA = 3000 m and ELA = 3100 m. In Fig. B1b and B1c, we show the corresponding glacier thickness $H$ and velocity $u$ during the retreat. Note that for driving stresses below the upper threshold (100 to 125 kPa) velocities drop to virtually zero (Fig B1c).

To illustrate the sensitivity of the model to variations in the thresholds, in Fig. B2 we rerun the experiments shown above in Fig. 6 but for different values of lower threshold $\tau_d^-$ while keeping constant $\tau_d^+ = 125$ kPa and $\lambda_m = 10\%$. For larger values of the lower threshold $\tau_d^-$, the full effect of cryokarst is felt sooner and therefore the volume and length response occur sooner (Fig. B2). However, the percentage of bare ice equivalent, shown in Fig. B2c, is less for larger $\tau_d^-$ values as the zone of stagnation driven cryokarst has less time to develop.

https://doi.org/10.5194/tc-2020-228
Preprint. Discussion started: 21 September 2020




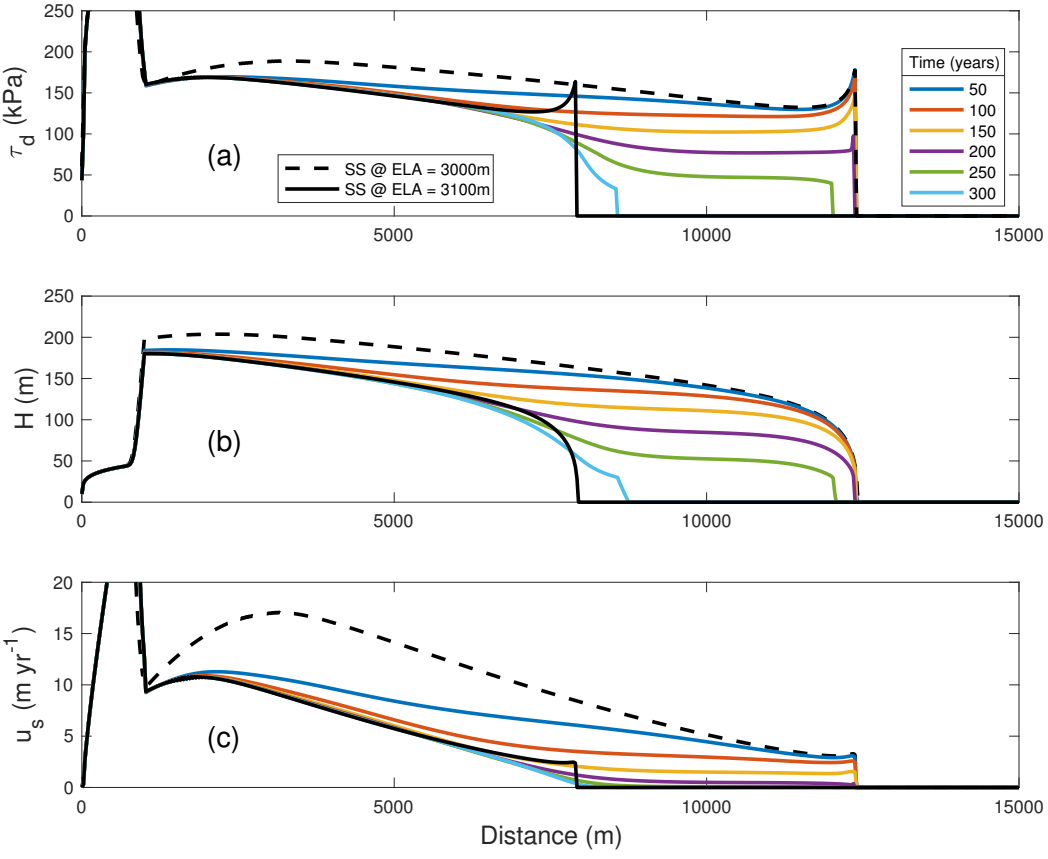


**Figure B1.** Effect of glacier retreat in response to step change in ELA on profiles of (a) driving stress $\tau_d$, (b) ice thickness $H$, and surface velocity $u_s$ at time intervals of 50 yr.

https://doi.org/10.5194/tc-2020-228
Preprint. Discussion started: 21 September 2020


The Cryosphere Discussions
Open Access
EGU

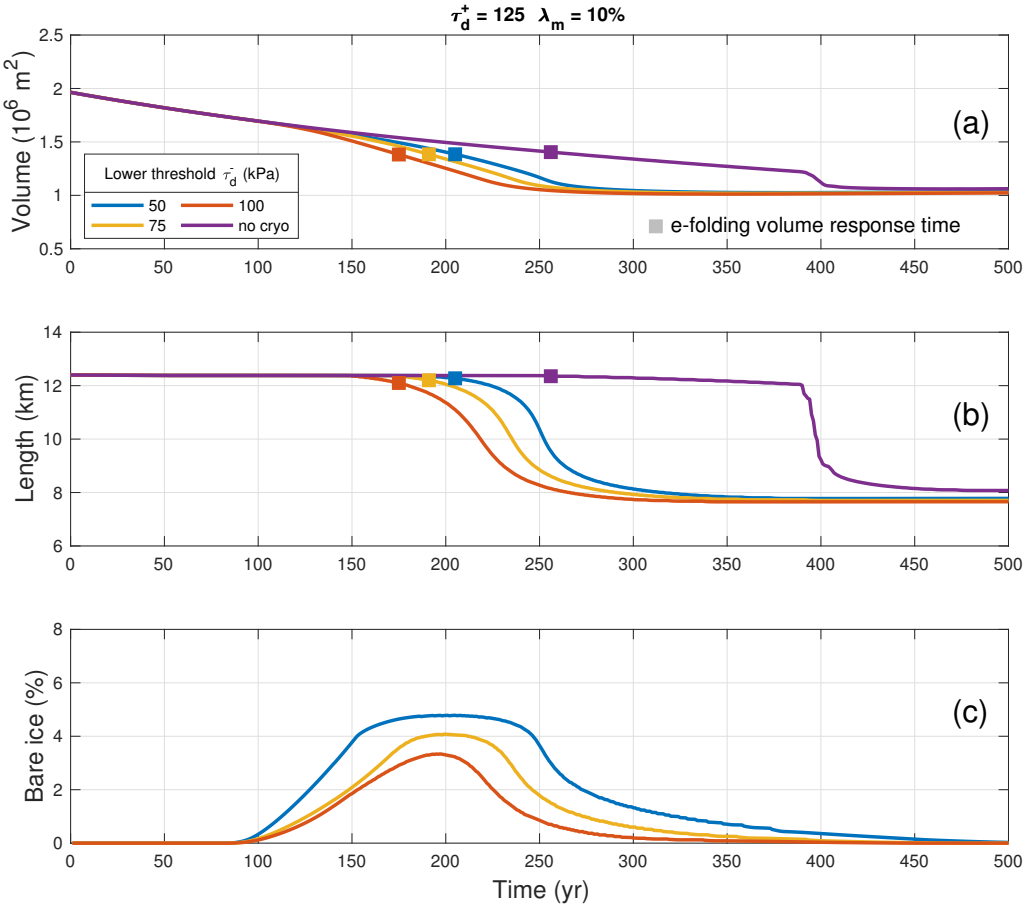


**Figure B2.** Sensitivity of model to different lower threshold values $\tau_d^-$ shown by coloured lines for (a) transient volume response, (b) transient length response and (c) bare ice equivalent debris-covered area during a retreat after a 100 m step change in ELA. In all cases, the debris concentration is $c = 0.25\%$, the upper driving stress threshold is $\tau_d^+ = 125$ kPa, and the maximum cryokarst fraction is $\lambda_m = 10\%$.

https://doi.org/10.5194/tc-2020-228
Preprint. Discussion started: 21 September 2020


*Author contributions.* JF and AV designed the study. JF wrote the code and performed the numerical experiments. JF interpreted the data and wrote the paper with input from AV.

*Competing interests.* None.

*Acknowledgements.* We thank Tobias Bolch and Nico Mölg for helpful discussions. This research was financially supported by the Swiss National Science Foundation grant number 169775, entitled “Understanding and quantifying the transient dynamics and evolution of debris-covered glaciers".

https://doi.org/10.5194/tc-2020-228
Preprint. Discussion started: 21 September 2020




## References

Anderson, L., Armstrong, W., Anderson, R., and Buri, P.: Debris cover and the thinning of Kennicott Glacier, Alaska, Part C: feedbacks between melt, ice dynamics, and surface processes, The Cryosphere Discussions, pp. 1–25, https://doi.org/10.5194/tc-2019-178, 2019a.

Anderson, L., Armstrong, W., Anderson, R., and Buri, P.: Debris cover and the thinning of Kennicott Glacier, Alaska, Part B: ice cliff delineation and distributed melt estimates, The Cryosphere Discussions, pp. 1–29, https://doi.org/10.5194/tc-2019-177, 2019b.

Anderson, L. S. and Anderson, R. S.: Modeling debris-covered glaciers: Response to steady debris deposition, The Cryosphere, 10, 1105–1124, https://doi.org/10.5194/tc-10-1105-2016, 2016.

Anderson, L. S. and Anderson, R. S.: Debris thickness patterns on debris-covered glaciers, Geomorphology, 311, 1–12, https://doi.org/10.1016/j.geomorph.2018.03.014, 2018.

Bahr, D. B., Meier, M. F., and Peckham, S. D.: The physical basis of glacier volume-area scaling, Journal of Geophysical Research: Solid Earth, 102, 20 355–20 362, https://doi.org/10.1029/97JB01696, http://doi.wiley.com/10.1029/97JB01696, 1997.

Banerjee, A. and Shankar, R.: On the response of Himalayan glaciers to climate change, Journal of Glaciology, 59, 480–490, https://doi.org/10.3189/2013JoG12J130, 2013.

Benn, D. I., Bolch, T., Hands, K., Gulley, J., Luckman, A., Nicholson, L. I., Quincey, D., Thompson, S., Toumi, R., and Wiseman, S.: Response of debris-covered glaciers in the Mount Everest region to recent warming, and implications for outburst flood hazards, Earth-Science Reviews, 114, 156–174, https://doi.org/10.1016/j.earscirev.2012.03.008, 2012.

Bolch, T., Kulkarni, A., Kääb, A., Huggel, C., Paul, F., Cogley, J. G., Frey, H., Kargel, J. S., Fujita, K., Scheel, M., Bajracharya, S., and Stoffel, M.: The state and fate of himalayan glaciers, Science, 336, 310–314, https://doi.org/10.1126/science.1215828, 2012.

Brun, F., Buri, P., Miles, E. S., Wagnon, P., Steiner, J., Berthier, E., Ragettli, S., Kraaijenbrink, P., Immerzeel, W. W., and Pellicciotti, F.: Quantifying volume loss from ice cliffs on debris-covered glaciers using high-resolution terrestrial and aerial photogrammetry, Journal of Glaciology, 62, 684–695, https://doi.org/10.1017/jog.2016.54, 2016.

Brun, F., Wagnon, P., Berthier, E., Shea, J. M., Immerzeel, W. W., Kraaijenbrink, P. D., Vincent, C., Reverchon, C., Shrestha, D., and Arnaud, Y.: Ice cliff contribution to the tongue-wide ablation of Changri Nup Glacier, Nepal, central Himalaya, The Cryosphere, 12, 3439–3457, https://doi.org/10.5194/tc-12-3439-2018, 2018.

Buri, P., Miles, E. S., Steiner, J. F., Immerzeel, W. W., Wagnon, P., and Pellicciotti, F.: A physically based 3-D model of ice cliff evolution over debris-covered glaciers, Journal of Geophysical Research: Earth Surface, 121, 2471–2493, https://doi.org/10.1002/2016JF004039, 2016.

Escher von der Linth, H. K.: Lauteraargletscher am Grimsel, https://doi.org/https://doi.org/10.7891/e-manuscripta-49948, 1794.

Gardelle, J., Berthier, E., Arnaud, Y., and Kääb, A.: Region-wide glacier mass balances over the Pamir-Karakoram-Himalaya during 1999–2011, Cryosphere, 7, 1263–1286, https://doi.org/10.5194/tc-7-1263-2013, 2013.

Harrison, W. D., Elsberg, D. H., Echelmeyer, K. A., and Krimmel, R. M.: On the characterization of glacier response by a single time-scale, Journal of Glaciology, 47, 659–664, https://doi.org/10.3189/172756501781831837, 2001.

Jóhannesson, T., Raymond, C., and Waddington, E.: Time-scale for adjustment of glaciers to changes in mass balance, Journal of Glaciology, 35, 355–369, https://doi.org/10.1017/S002214300000928X, 1989.

Kääb, A., Berthier, E., Nuth, C., Gardelle, J., and Arnaud, Y.: Contrasting patterns of early twenty-first-century glacier mass change in the Himalayas, Nature, 488, 495–498, https://doi.org/10.1038/nature11324, 2012.

https://doi.org/10.5194/tc-2020-228
Preprint. Discussion started: 21 September 2020


Kirkbride, M. P.: Debris-Covered Glaciers, in: Encyclopedia of Snow, Ice and Glaciers, edited by Singh, V. P., Singh, P., and Haritashya, U. K., September, pp. 180–182, Springer, Dordrecht, https://doi.org/10.1007/978-90-481-2642-2_622, 2011.

Konrad, S. K. and Humphrey, N. F.: Steady-state flow model of debris-covered glaciers (rock glaciers), IAHS-AISH Publication, pp. 255–263, 2000.

Leysinger Vieli, G. J.-M. C. and Gudmundsson, G. H.: On estimating length fluctuations of glaciers caused by changes in climatic forcing, Journal of Geophysical Research: Earth Surface, 109, 1–14, https://doi.org/10.1029/2003jf000027, 2004.

Linsbauer, A., Paul, F., Machguth, H., and Haeberli, W.: Comparing three different methods to model scenarios of future glacier change in the Swiss Alps, Annals of Glaciology, 54, 241–253, https://doi.org/10.3189/2013AoG63A400, 2013.

Mahaffy, M. W.: A three-dimensional numerical model of ice sheets: Tests on the Barnes Ice Cap, Northwest Territories, Journal of Geophysical Research, 81, 1059–1066, https://doi.org/10.1029/JC081i006p01059, http://doi.wiley.com/10.1029/JC081i006p01059, 1976.

Miles, E. S., Pellicciotti, F., Willis, I. C., Steiner, J. F., Buri, P., and Arnold, N. S.: Refined energy-balance modelling of a supraglacial pond, Langtang Khola, Nepal, Annals of Glaciology, 57, 29–40, https://doi.org/10.3189/2016AoG71A421, 2016.

Mölg, N., Bolch, T., Walter, A., and Vieli, A.: Unravelling the evolution of Zmuttgletscher and its debris cover since the end of the Little Ice Age, The Cryosphere, 13, 1889–1909, https://doi.org/10.5194/tc-13-1889-2019, 2019.

Mölg, N., Ferguson, J., Bolch, T., and Vieli, A.: On the influence of debris cover on glacier morphology: How high-relief structures evolve from smooth surfaces, Geomorphology, 357, 107 092, https://doi.org/10.1016/j.geomorph.2020.107092, https://doi.org/10.1016/j.geomorph.2020.107092, 2020.

Naito, N., Nakawo, M., Kadota, T., and Raymond, C. F.: Numerical simulation of recent shrinkage of Khumbu Glacier, Nepal Himalayas, IAHS-AISH Publication, m, 245–254, 2000.

Nicholson, L. and Benn, D. I.: Calculating ice melt beneath a debris layer using meteorological data, Journal of Glaciology, 52, 463–470, https://doi.org/10.3189/172756506781828584, 2006.

Ogilvie, I. H.: The Effect of Superglacial Débris on the Advance and Retreat of Some Canadian Glaciers, The Journal of Geology, 12, 722–743, https://doi.org/10.1086/621194, 1904.

Østrem, G.: Ice Melting under a Thin Layer of Moraine, and the Existence of Ice Cores in Moraine Ridges, Geografiska Annaler, 41, 228–230, https://doi.org/10.1080/20014422.1959.11907953, 1959.

Pellicciotti, F., Stephan, C., Miles, E., Herreid, S., Immerzeel, W. W., and Bolch, T.: Mass-balance changes of the debris-covered glaciers in the Langtang Himal, Nepal, from 1974 to 1999, Journal of Glaciology, 61, 373–386, https://doi.org/10.3189/2015JoG13J237, 2015.

Quincey, D. J., Luckman, A., and Benn, D.: Quantification of Everest region glacier velocities between 1992 and 2002, using satellite radar interferometry and feature tracking, Journal of Glaciology, 55, 596–606, https://doi.org/10.3189/002214309789470987, 2009.

Ragettli, S., Bolch, T., and Pellicciotti, F.: Heterogeneous glacier thinning patterns over the last 40 years in Langtang Himal, Nepal, The Cryosphere, 10, 2075–2097, https://doi.org/10.5194/tc-10-2075-2016, 2016.

Rounce, D. R., King, O., McCarthy, M., Shean, D. E., and Salerno, F.: Quantifying Debris Thickness of Debris-Covered Glaciers in the Everest Region of Nepal Through Inversion of a Subdebris Melt Model, Journal of Geophysical Research: Earth Surface, 123, 1094–1115, https://doi.org/10.1029/2017JF004395, 2018.

Rowan, A. V., Egholm, D. L., Quincey, D. J., and Glasser, N. F.: Modelling the feedbacks between mass balance, ice flow and debris transport to predict the response to climate change of debris-covered glaciers in the Himalaya, Earth and Planetary Science Letters, 430, 427–438, https://doi.org/10.1016/j.epsl.2015.09.004, 2015.

https://doi.org/10.5194/tc-2020-228
Preprint. Discussion started: 21 September 2020


Sakai, A., Takeuchi, N., Fujita, K., and Nakawo, M.: Role of supraglacial ponds in the ablation process of a debris-covered glacier in the Nepal Himalayas, IAHS-AISH Publication, pp. 119–130, 2000.

Sakai, A., Nakawo, M., and Fujita, K.: Distribution Characteristics and Energy Balance of Ice Cliffs on Debris-covered Glaciers, Nepal Himalaya, Arctic, Antarctic, and Alpine Research, 34, 12–19, https://doi.org/10.1080/15230430.2002.12003463, 2002.

Scherler, D., Bookhagen, B., and Strecker, M. R.: Spatially variable response of Himalayan glaciers to climate change affected by debris cover, Nature Geoscience, 4, 156–159, https://doi.org/10.1038/ngeo1068, 2011.

Steiner, J. F., Pellicciotti, F., Buri, P., Miles, E. S., Immerzeel, W. W., and Reid, T. D.: Modelling ice-cliff backwasting on a debris-covered glacier in the Nepalese Himalaya, Journal of Glaciology, 61, 889–907, https://doi.org/10.3189/2015JoG14J194, 2015.

Steiner, J. F., Buri, P., Miles, E. S., Ragettli, S., and Pellicciotti, F.: Supraglacial ice cliffs and ponds on debris-covered glaciers: Spatio-temporal distribution and characteristics, Journal of Glaciology, 65, 617–632, https://doi.org/10.1017/jog.2019.40, 2019.

Vacco, D. A., Alley, R. B., and Pollard, D.: Glacial advance and stagnation caused by rock avalanches, Earth and Planetary Science Letters, 294, 123–130, https://doi.org/10.1016/j.epsl.2010.03.019, 2010.